Error thresholds for Abelian quantum double models: Increasing the bit-flip stability of topological quantum memory

Ruben S. Andrist, James R. Wootton, and Helmut G. Katzgraber

Phys. Rev. A **91**, 042331 — Published 24 April 2015

DOI: 10.1103/PhysRevA.91.042331

Error Thresholds for Abelian Quantum Double Models: Increasing the bit-flip Stability of Topological Quantum Memory

Ruben S. Andrist,[1] James R. Wootton,[2] and Helmut G. Katzgraber[3,4,1]

[1]*Santa Fe Institute, 1399 Hyde Park Road, Santa Fe, NM 87501*
[2]*Department of Physics, University of Basel, Klingelbergstrasse 82, CH-4056 Basel, Switzerland*
[3]*Department of Physics and Astronomy, Texas A&M University, College Station, Texas 77843-4242, USA*
[4]*Materials Science and Engineering Program, Texas A&M University, College Station, Texas 77843, USA*

Current approaches for building quantum computing devices focus on two-level quantum systems which nicely mimic the concept of a classical bit, albeit enhanced with additional quantum properties. However, rather than artificially limiting the number of states to two, the use of d-level quantum systems (qudits) could provide advantages for quantum information processing. Among other merits, it has recently been shown that multi-level quantum systems can offer increased stability to external disturbances. In this study we demonstrate that topological quantum memories built from qudits, also known as abelian quantum double models, exhibit a substantially increased resilience to noise. That is, even when taking into account the multitude of errors possible for multi-level quantum systems, topological quantum error correction codes employing qudits can sustain a larger error rate than their two-level counterparts. In particular, we find strong numerical evidence that the thresholds of these error-correction codes are given by the hashing bound. Considering the significantly increased error thresholds attained, this might well outweigh the added complexity of engineering and controlling higher dimensional quantum systems.

I. INTRODUCTION

The prospect of tremendous speedup over classical computation has channeled considerable research effort into the pursuit of building a universal quantum computer [1, 2]. However, one of the most significant challenges has been error correction: Despite numerous attempts to physically realize and control quantum bits, all share a striking sensitivity to decoherence – external disturbance attributed to the unavoidable interaction with the environment. And while correcting these errors is in principle possible [3, 4], achieving error resilience in an efficient and, in particular, scalable way is challenging and consequently a topic of considerable research interest.

Traditionally, quantum information processing is conceptualized as a quantum adaptation of the binary storage system found in current computers. However, there are several indicators that "thinking outside the binary box" might be a key ingredient to further progress towards reliable quantum computation. Recent results suggest that d-level quantum systems, so called "qudits," are potentially more powerful than their binary counterparts in terms of information processing [5–9]. Furthermore, while single-qubit gates can typically be implemented with relatively high fidelity, two-qubit gates are often more challenging because they require concurrent control over several parts of the system. Higher-dimensional quantum systems can allow for information-coding with increased density, thus potentially reducing the number of error-prone inter-qudit interactions required to perform specific computations [10].

Different working quantum computing devices are currently being scrutinized by a myriad of research teams around the globe: These range from superconducting flux qubits, to trapped ions that recently demonstrated successfully fault-tolerant quantum computation based on topological protection [11]. While the former is built for scalability, it suffers from decoherence effects mostly due to $1/f$ noise. The latter, on the other hand, is robust against noise due to the inherent topological protection, however shows little prospect of scalability. Several of the current approaches to physically represent quantum information can be extended to more than two levels, including optical system [12, 13], superconductors and flux qubits [14], as well as atomic spins [15, 16]. Given the theoretical promise that qudit-based systems have shown [5–7], it is thus of paramount interest to quantify their resilience to noise.

In terms of achieving error resilience for a given set of building blocks, topological error-correction codes are currently among the best candidates for a scalable error-correction scheme [17, 18]. This approach of using topology to reliably encode quantum information can also be extended to multi-level qudit systems, resulting in the so-called abelian quantum double models [19]. We are interested in estimating the dependence of the error threshold on the qudit dimensionality – that is, the maximum amount of errors a system of d-level qudits can sustain while still being able to reliably store the encoded information. In the spirit of the approach used to estimate the error tolerance of fault-tolerant systems pioneered in Refs. [20–22] for qubit and qutrit systems, we present a mapping of this statistical analysis to classical Potts gauge glasses that can be seen as the natural extension of Boolean (two-level) variables to d-level states. This allows us to numerically calculate the bit-flip error threshold for qudit-based quantum memories using Monte Carlo simulations, a key figure of merit. This is the threshold that would arise for *optimal* decoding methods, and is an important benchmark in the study of error correction.

The paper is structured as follows. In Sec. II we introduce abelian quantum double models, followed by both upper and lower theoretical bounds for the threshold. A mapping onto a statistical mechanical Potts gauge glass is outlined in Sec. III, followed by results in Sec. IV and concluding remarks.

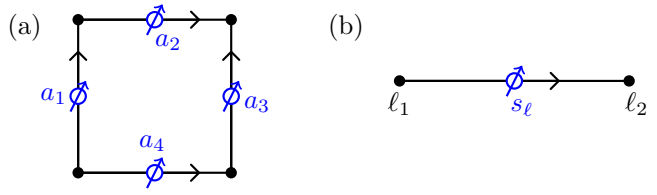

FIG. 1: Numbering and orientation conventions used in the calculations. The quantum spins of the original model are shown as (blue) empty circles on the graph's edges, whereas the sites of the classical model are shown as (black) solid dots on the vertices. (a) Convention for determining anyon occupancy of a plaquette $\square$ from the quantum spins on the edges. (b) Convention for assigning classical spins S_{ℓ_1} and S_{ℓ_2} to the vertices and determining the effective κ_ℓ for a given link ℓ.

II. ABELIAN QUANTUM DOUBLE MODELS

The abelian quantum double models are defined on a square lattice with a d-level quantum spin on each edge ℓ. Let us use $|\, s_\ell\rangle \in \{|\, 0\rangle, \ldots, |\, d-1\rangle\}$ to denote the computational basis of the spins. We will use these to define a qudit generalization of the toric code based on the cyclic group $\mathbb{Z}_d$, which we call the $D(\mathbb{Z}_d)$ code [17].

Like the qubit-based toric code, operators are defined on the spins around each plaquette and vertex of a square lattice in order to define occupancies of anyonic quasiparticles. For the plaquettes, these operators depend on relations between the states of the spins around the plaquette when expressed in the computational basis. In the case that all the spins $\square_j$ around a plaquette $\square$ are in definite computational basis states $\left|\, s_{\square_j}\right\rangle$, the plaquette is said to hold an anyon of type $n_\square$, where

$$n_\square = (s_{\square_1} + s_{\square_2} - s_{\square_3} - s_{\square_4}) \mod d\,. \tag{1}$$

The numbering of the spins in Eq. (1) around the plaquette is depicted in Fig. 1(a). The $n = 0$ anyon is identified with the vacuum, while the $d-1$ other anyon types are non-trivial. Note that many different states for the spins around a plaquette lead to the same anyon type contained within. The typical states of the system with a given anyon configuration will correspond to a superposition of many of these.

The plaquette anyons can be created, moved, and annihilated using the operations

$$(\sigma_\ell^x)^\epsilon = \sum_{s_\ell} |\, s_\ell + \epsilon \mod d\rangle \langle s_\ell\,|\,. \tag{2}$$

There are d distinct operations given by $\epsilon \in \{0, \ldots, d-1\}$. All are non-trivial except $\epsilon = 0$, which yields the identity.

For the vertices of the code anyon occupancies are defined in a similar manner as for the plaquettes. The basis used is not the computational basis, but that defined by

$$|\,\tilde{j}\rangle = \frac{1}{\sqrt{d}} \sum_{k=0}^{d-1} e^{i2\pi jk/d}\, |\, j\rangle\,. \tag{3}$$

There are also corresponding operations $(\sigma_\ell^z)^\epsilon$ that manipulate these anyons. These vertex anyons are completely dual to the plaquette ones, and so can be treated independently and analogously. We therefore restrict our attention to plaquette anyons without loss of generality.

Quantum information is stored in the vacuum states of the anyons, i.e., states where no anyons are present on any plaquette or vertex. There are d such states, allowing a logical qudit to be stored. The action of any errors on the code can be expressed in terms of the $(\sigma_\ell^x)^\epsilon$ and $(\sigma_\ell^z)^\epsilon$ operations, and so correspond to the creation and manipulation of anyons. The resulting anyon configuration, which serves as the syndrome of the code, then allows information about the errors to be determined. The goal of error correction is to use this information to remove the effects of the errors.

Error correction will not always succeed. The probability with which it fails depends on the linear system size of the code, L, and the strength of the noise, p. If p is below a threshold value, which we denote p_d for a $D(\mathbb{Z}_d)$ code, the probability of failure decays exponentially with L. Success then become certain as $L \to \infty$. For $p > p_d$, however, the probability of failure is always $O(1)$.

To determine the value of the error threshold p_d for a $D(\mathbb{Z}_d)$ code, we must consider a specific error model. Here we consider a generalization of the well-known independent bit and phase flip error model for the $\mathbb{Z}_2$ case [20]. This acts independently on each spin of the code, applying a randomly chosen non-trivial operation $(\sigma_\ell^x)^\epsilon$ with probability p. The probability of each non-trivial operation is therefore $p/(d-1)$.

The value of the error threshold depends also strongly on the method used to determine how to attempt to remove the errors, given the information provided by the syndrome. Such methods are known as decoding algorithms. The optimal algorithm would provide maximum likelihood decoding, which uses the syndrome to determine which correction method will succeed with the highest probability. The threshold found using such a method would be the one intrinsic to the capabilities of the code. As such, it is this threshold that can be found by studying the underlying statistical mechanics problem. However, such methods are typically inefficient. Algorithms that run in a time that is polynomial with the code size are instead preferable. These realize an effective threshold that will be lower than the intrinsic one in general. The trade-off between the speed and threshold of a decoder is therefore one of the most important factors in designing decoding algorithms. See Refs. [23–25] for the best efficient decoding algorithms for this problem to date. Henceforth we will use 'threshold' to refer only to intrinsic thresholds unless otherwise stated.

In Sec. IV, the thresholds are determined numerically for several different values of d. However it is interesting to consider how p_d may behave for $d \to \infty$.

For the $\mathbb{Z}_2$ code it has been observed in multiple cases that the threshold follows the Hashing bound [26, 27]. It has been conjectured that this may also hold in the qudit case [23, 24], based on findings that effective thresholds follow the same scaling as the Hashing bound would predict for increasing d. For the error model we consider, the Hashing bound probabil-

ity $p_{\rm hb}$ is the solution to the equation

$$p_{\rm hb}\log(d-1)-p_{\rm hb}\log p_{\rm hb}-(1-p_{\rm hb})\log(1-p_{\rm hb})=\frac{\log d}{2}\,. \tag{4}$$

This bound is a consequence of the Lloyd-Shor-Devetak theorem [28, 29], which does not strictly apply to the codes we consider. As such, the thresholds for these codes are not necessarily limited by these values.

A. Upper bound for thresholds

Even though the Hashing bound is not a strict upper bound for the codes we consider, such a bound can be derived. Suppose all spins of a $D(\mathbb{Z}_d)$ code are prepared in state $|\,0\rangle$. If the anyon configuration is then measured, it will be found that there is only vacuum on all plaquettes but a random pattern of anyons on the vertices. When the latter are removed, the resulting state of the code is that for which the logical qubit state is $|\,0\rangle$.

Now suppose that a unitary $U(\theta)$ is applied to all spins prior to the measurement, such that

$$U(\theta)\,|\,0\rangle=\cos\theta\,|\,0\rangle+\sin\theta\frac{1}{\sqrt{d-1}}\sum_{j=1}^{d-1}|\,j\rangle\,. \tag{5}$$

This has the same effects on the measurement results as applying errors of the form $(\sigma^x)^g$ for $1\le g\le d-1$ with equal probability $p/(d-1)$, where $p=\sin^2\theta$. The threshold p_d in the latter case therefore corresponds to a threshold angle $\theta_d=\arcsin\sqrt{p}_d$ in the former. For $\theta<\theta_d$ error correction will yield the code in logical state $|\,0\rangle$ with certainty as $L\to\infty$.

A similar argument can be applied using the complementary basis in which the vertex anyon states are defined. If each qudit is prepared in state $\big|\,\tilde{0}\big\rangle$, syndrome measurement and error correction result in the logical qubit state $\big|\,\tilde{0}\big\rangle$. Applying the unitary operator

$$V(\phi)\,\big|\,\tilde{0}\big\rangle=\cos\phi\,\big|\,\tilde{0}\big\rangle+\sin\phi\frac{1}{\sqrt{d-1}}\sum_{j=1}^{d-1}\big|\,\tilde{j}\big\rangle \tag{6}$$

to each spin before measurement has the same effect as errors of the form $(\sigma^z)^g$ for $1\le g\le d-1$ with equal probability $p/(d-1)$ where $p=\sin^2\phi$. There will then be a critical angle $\phi_d=\arcsin\sqrt{p}_d$ below which error correction yields the code in logical state $\big|\,\tilde{0}\big\rangle$ with certainty as $L\to\infty$.

Note that, for particular values of θ and ϕ,

$$U(\theta)\,|\,0\rangle=V(\phi)\,\big|\,\tilde{0}\big\rangle=\sqrt{\frac{d}{2(d+\sqrt{d})}}\left(|\,0\rangle+\big|\,\tilde{0}\big\rangle\right)\,. \tag{7}$$

This corresponds to both of the above cases with the errors occurring with probability

$$p=\frac{d-1}{2(d+\sqrt{d})}. \tag{8}$$

As such, error correction cannot successfully correct both types of error, because it cannot yield a code whose logical state is simultaneously $|\,0\rangle$ and $\big|\,\tilde{0}\big\rangle$. This error rate must therefore be above the threshold, giving us an upper bound

$$p_d<\frac{d-1}{2(d+\sqrt{d})} \tag{9}$$

for the threshold error rate p_d of the $D(\mathbb{Z}_d)$ code.

B. Lower bound for thresholds

For some values of d it is also possible to construct a lower bound: Given an integer $d=nm$ where n and m are co-prime, the fundamental theorem of abelian groups states that the group $\mathbb{Z}_d$ is isomorphic to $\mathbb{Z}_n\times\mathbb{Z}_m$. As such, the problem of decoding an error correcting code based on the $D(\mathbb{Z}_d)$ quantum double model is the same as that for two separate codes, one based on $D(\mathbb{Z}_n)$ and the other on $D(\mathbb{Z}_m)$. We may therefore consider the independent decoding of these two component codes, rather than decoding the full $D(\mathbb{Z}_d)$ code.

By definition, the optimal decoding of the component codes cannot do better than optimal decoding for the full $D(\mathbb{Z}_d)$ code. In general it will do worse, because the error model for the full $D(\mathbb{Z}_d)$ code will translate to one on the component codes with strong correlations between the two. Ignoring these correlations by decoding the component codes independently leads to decreased performance.

For the $D(\mathbb{Z}_d)$ code there are $d-1$ non-trivial errors of the form $(\sigma^x)^g$, corresponding to $0<g\le d-1$. The number of these that act non-trivially on the $\mathbb{Z}_n$ code is $(n-1)m$: the number of elements of $\mathbb{Z}_n\times\mathbb{Z}_m$ that do not correspond to the identity for $\mathbb{Z}_n$. These all occur with equal probability $p/(d-1)$. Using $p^{(n)}$ to denote the total probability of error for the $\mathbb{Z}_n$ code, it follows

$$\frac{p^{(n)}}{(n-1)m}=\frac{p}{d-1},\quad\therefore\quad p=p^{(n)}\,\frac{d-1}{d-m}\,.$$

When decoding the component codes independently, error correction fails when either of the component codes experience an error rate above their threshold. The error rate p at which this occurs is then a lower bound for p_d, i.e.,

$$p_d\ge\min\left(p_n\,\frac{d-1}{d-m},p_m\,\frac{d-1}{d-n}\right)\overset{n<m}{\ge}p_n\,\frac{d-1}{d-n}\,.$$

We can also use this as a self-consistency check for any proposed set of thresholds $p_d^{\rm prop}$, such as those provided by the hashing bound, Eq. (4). The easiest way to do this is to use prime n, ensuring that $m=n+1$ is co-prime. Self-consistency then requires

$$p^{\rm prop}_{n^2+n}\ge p^{\rm prop}_n\left(1+\frac{1}{n}-\frac{1}{n^2}\right)\,,$$

which is indeed satisfied by the hashing bound values.

III. MAPPING AND NUMERICAL SIMULATIONS

We first map the problem of computing the error threshold to a classical statistical-mechanical model with disorder. The threshold where errors in the quantum setup cannot be corrected any longer will correspond to the loss of a symmetry broken phase in the classical model.

A. Mapping

For the mapping we consider a square lattice and an initially anyon-free state, $n_\square = 0\,\forall\square$. Errors $(\sigma_\ell^x)^{\epsilon_\ell}$ are applied independently to each quantum spin, where ϵ_ℓ denotes the type of error applied to the spin on edge ℓ. We initially perform the mapping with a general error model where each value occurs with respective probability p_ϵ and the error is non-trivial with total probability $p = \sum_{\epsilon\neq 0} p_\epsilon$. The probability for a given error configuration $E = \{\epsilon_l\}$ is then

$$P(E) = \prod_\ell \prod_\epsilon p_\epsilon^{\delta_{\epsilon_\ell,\epsilon}} = \prod_\ell \exp[-\beta \sum_\epsilon J_\epsilon \delta_{\epsilon_\ell,\epsilon}]\,, \qquad (10)$$

where β, J_ϵ and p_ϵ satisfy

$$p_\epsilon = e^{-\beta J_\epsilon}\,. \qquad (11)$$

Assuming an initially anyon free state, the set of errors E yields an anyon configuration with the type of the anyon on plaquette $\square$ given by

$$n_\square^E = \epsilon_{\square_1} + \epsilon_{\square_2} - \epsilon_{\square_3} - \epsilon_{\square_4} \mod d\,.$$

Let us now consider another set of errors $E' = \{\epsilon'_\ell\}$. This can be related to E by a third set $C = \{\kappa_\ell\}$ according to

$$\epsilon'_\ell = \epsilon_\ell + \kappa_\ell \mod d\,.$$

Note that if E and E' lead to the same anyon configuration, $n_\square^E = n_\square^{E'}$, then the anyon configuration of C is trivial. Explicitly, it satisfies

$$n_\square^C = (\kappa_{\square_1} + \kappa_{\square_2} - \kappa_{\square_3} - \kappa_{\square_4}) \mod d = 0\ \forall\square\,. \qquad (12)$$

This follows from the fact that $\kappa_\ell = \epsilon'_\ell - \epsilon_\ell$, and hence $n_\square^C = n_\square^{E'} - n_\square^E = 0$ (both evaluated $\mod d$). Combining Eqs. (10) and (12), we find that the ratio of the probabilities for E' and E can be written as

$$\frac{P(E')}{P(E)} = \prod_\ell \exp[-\beta \sum_\epsilon J_\epsilon(\delta_{\epsilon_\ell+\kappa_\ell,\epsilon} - \delta_{\epsilon_\ell,\epsilon})]\,,$$

where the sum $\epsilon_\ell + \kappa_\ell$ is again evaluated $\mod d$. This ratio can be interpreted as a Boltzmann weight for a classical model with the Hamiltonian

$$\mathcal{H} = \sum_\ell \sum_\epsilon J_\epsilon(\delta_{\epsilon_\ell+\kappa_\ell,\epsilon} - \delta_{\epsilon_\ell,\epsilon})\,. \qquad (13)$$

We interpret the $\{\kappa_\ell\}$ as the state of the system and $\{\epsilon_\ell\}$ as representing the details of the (quenched) interactions. Because the partition function sums only over the former, the second term in the brackets of Eq. (13) is an overall constant and hence can be ignored.

To ensure that E and E' belong to the same error class, we require that a system state $\{\kappa_\ell\}$ satisfies the constraint in Eq. (12). This is achieved by introducing an auxiliary d-level classical spin $S_v \in \{0,\ldots,d-1\}$ on each vertex v of the lattice. The κ_ℓ can then be defined by $\kappa_\ell = S_{\ell_2} - S_{\ell_1}$ with the numbering as indicated in Fig. 1(b). All the S_v around a plaquette $\square$ will then appear exactly twice in $n_\square^C$ (and with opposite sign), thus leaving the required value of zero in all cases.

In summary, we can sample from the set of errors E' with the same anyon configuration as a set E (i.e., from the *error class* of E) by sampling from a classical two-dimensional statistical-mechanical spin model defined on a square lattice with $N = L \times L$ sites and d-level spins on the vertices. The classical spin model of interest has the Hamiltonian

$$\mathcal{H}(E) = \sum_\ell \sum_\epsilon J_\epsilon \delta_{\epsilon_\ell + S_{\ell_1} - S_{\ell_2},\epsilon}\,, \qquad (14)$$

where the errors of $E = \{\epsilon_\ell\}$ are generated according to the error model. The inverse temperature β and the interaction constants J_ϵ need to be scaled accordingly to satisfy Eq. (11).

For the purpose of our numerical simulations, we consider the special case where all non-trivial errors have equal probability: $p_\epsilon = p/(d-1)\ \forall\epsilon \neq 0$. In this case the simplest way to satisfy Eq. (11) is to sample at inverse temperature

$$\beta = -\ln \frac{p/(d-1)}{1-p}\,. \qquad (15)$$

This is the generalization of the Nishimori condition [30], which, for the symmetrical case, ensures that the Boltzmann weight of each state corresponds to the a priori probability of the quantum error configuration it represents. The spin Hamiltonian, up to an irrelevant overall energy shift, then takes the form

$$\mathcal{H}(E) = -\sum_\ell \delta_{\epsilon_\ell + S_{\ell_q} - S_{\ell_2},0}\,, \qquad (16)$$

which can be interpreted as a disordered d-states Potts gauge glass (see Fig. 2 for a graphical illustration). In the mapping each quantum error is translated to a non-trivial interaction constant ϵ_ℓ and the difference is associated with the surface of a flipped domain of Potts spins. Therefore, if in our sampling we find the system in an overall ordered state, there is little uncertainty in the type of error that occurred. If by contrast the system is disordered, then the domain walls have percolated the system and we are unable to correctly identify the class of the actual error.

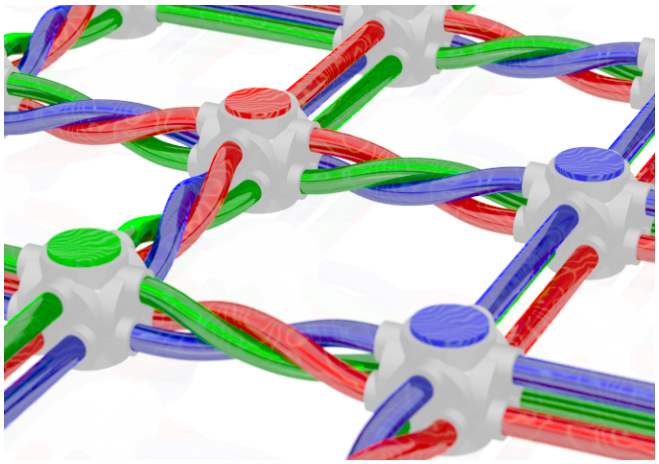

FIG. 2: (Color online) Rendering of the classical three-colored Potts gauge glass found in the mapping of an abelian quantum double model with qutrits (i.e., qubits with $d = 3$) on each edge. Quantum errors give rise to disorder in the interactions between neighboring sites, indicated in the form of twisted links. An ordered state in this model (i.e., one predominant color in the system) in spite of these faulty links indicates resilience of the original setup to quantum errors.

B. Numerical details: Algorithm & Observables

Algorithm — To calculate the error threshold (i.e., where ordering disappears), we numerically investigate Eq. (16) via large-scale (classical) Monte Carlo simulations using the parallel tempering technique [31]. Several replicas of the system are simulated concurrently for the same disorder realization, but at different temperatures $T = 1/\beta$. In addition to local Metropolis updates [32], one performs global moves in which the temperatures of two neighboring copies are exchanged. It is important to select the position of the individual temperatures carefully such that the acceptance probabilities for the global moves are large enough [33] and each copy performs a random walk in temperature space. This, in turn, allows each copy to efficiently sample the configuration space, therefore speeding up the simulation several orders of magnitude.

Observables — Detecting the transition temperature $T_c(p)$ to an ordered (ferromagnetic) phase for different fixed amounts of disorder p allows us to pinpoint the phase boundary in the p–T phase diagram. The error threshold p_c is then given by the intersection of the phase boundary with the Nishimori line, Eq. (15). To detect ordering, we use the simplex representation where the d states of the Potts spins are mapped to the corners of a hyper-tetrahedron in $(d-1)$ space dimensions. This means they are represented as a $(d-1)$-component unit vector $\mathbf{S}_i$ taking one of d possible values satisfying the condition $\mathbf{S}^\mu \cdot \mathbf{S}^\nu = 1 - \delta_{\mu,\nu}[d/(d-1)]$ with $\{\mu, \nu\} \in \{1, 2, \ldots, d\}$. Within this mapping, the magnetic susceptibility of the disordered Potts gauge glass in Eq. (16) can be computed via

$$\chi(\mathbf{k}) = \sum_{\mu} \left[\left\langle \left| \sum_i \mathbf{S}_i^\mu e^{i\mathbf{k}\cdot\mathbf{R}_i} \right|^2 \right\rangle \right]_{\mathrm{av}} , \tag{17}$$

TABLE I: Simulation parameters: d is the qudit dimensionality, p is the qudit error rate, L is the linear system size, N_{sa} is the number of disorder samples, $t_{\mathrm{eq}} = 2^b$ is the number of equilibration sweeps (system size times number of single-spin Monte Carlo updates), T_{min} [T_{max}] is the lowest [highest] temperature, and N_{T} the number of temperatures used.

d	p	L	N_{sa}	b	T_{min}	T_{max}	N_{T}
3, 4	0.00 – 0.13	12, 16	10 000	17	0.60	1.40	24
3, 4	0.00 – 0.13	24, 32	5 000	20	0.60	1.40	28
3, 4	0.00 – 0.13	48, 64	500	21	0.60	1.40	36
3, 4	0.15 – 0.19	12, 16	10 000	19	0.35	1.30	24
3, 4	0.15 – 0.19	24, 32	5 000	23	0.35	1.30	42
3, 4	0.15 – 0.19	48, 64	500	24	0.35	1.30	64
6, 10	0.00 – 0.20	12, 16	10 000	17	0.45	1.40	24
6, 10	0.00 – 0.20	24, 32	1 000	21	0.45	1.40	42
6, 10	0.21 – 0.26	12, 16	10 000	19	0.25	1.30	32
6, 10	0.21 – 0.26	24, 32	1 000	24	0.25	1.30	56

where the sum is over all Potts spins $\mathbf{S}_i$, $\langle \cdots \rangle$ denotes a thermal average and $[\cdots]_{\mathrm{av}}$ is an average over disorder realizations. The presence of a transition is probed by studying the two-point finite-size correlation length [34],

$$\xi_L = \frac{1}{2\sin(k_{\mathrm{min}}/2)} \sqrt{\frac{\chi(\mathbf{0})}{\chi(\mathbf{k}_{\mathrm{min}})} - 1} , \tag{18}$$

where $\mathbf{k}_{\mathrm{min}} = (2\pi/L, 0)$ is the smallest nonzero wave vector for the given lattice. Near the transition, ξ_L is expected to scale as

$$\xi_L/L \sim \tilde{X}[L^{1/\nu}(T - T_c)] , \tag{19}$$

where $\tilde{X}$ is a dimensionless scaling function. Because the argument of Eq. (19) becomes zero at the transition temperature (and hence independent of L), we expect lines of different system sizes to cross at this point. If however the lines do not meet, we know that no transition occurs in the studied temperature range. This approach has been successfully used before for qubit systems, see for example, Ref. [35].

Finite-size scaling — In practice, there are corrections to scaling to Eq. (19) and the data for different system sizes do not cross exactly at one temperature T_c as suggested by the finite-size scaling form, Eq. (19). That is, the actual crossing T_c^* between a pair of system sizes L_1 and L_2 shifts with increasing system size L and tends to a constant for L_1 and $L_2 \to \infty$. To estimate the proper thermodynamic value we study $T_c^*(L_1, L_2)$ as a function of the average inverse system size, $2/(L_1{+}L_2)$, and fit a linear function to the data [41]. The intercept with the vertical axis is our estimate for the transition temperature in the thermodynamic limit. The error bars are determined via a bootstrap analysis using 500 resamplings.

Thermalization — In all simulations, equilibration is tested using logarithmic binning of the data. Once the data for all observables measured agree within error bars for three logarithmic bins we deem the Monte Carlo simulation for that system size to be in thermal equilibrium. The detailed simulation parameters are listed in table I.

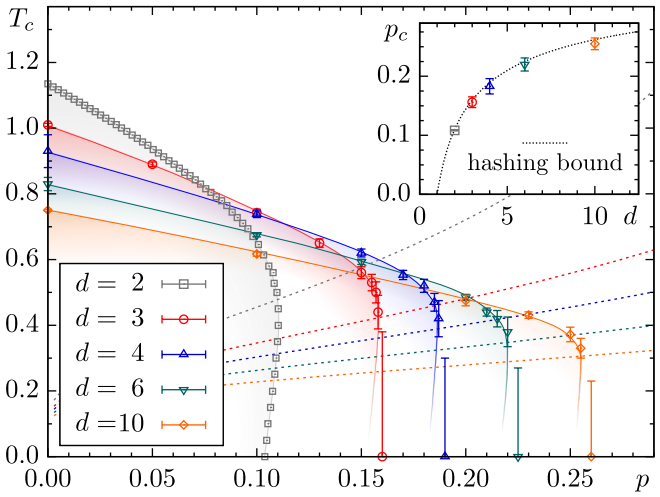

FIG. 3: (Color online) Phase boundaries for different d estimated from Monte Carlo simulations of the respective disordered Potts gauge glasses representing quantum error correction for d-level quantum systems. The solid lines and shaded areas are guides to the eye. The error threshold $p_c(d)$ corresponds to the point where the corresponding Nishimori line (dashed) intersects the phase boundary for a given d. This is the maximum disorder rate for which error correction is feasible. Inset: Comparison of the calculated error thresholds for different values of d to the hashing bound (dotted black line). There is excellent agreement. (Data for $d = 2$ are reproduced from Ref. 36.)

IV. RESULTS

In the mapping, the special case of $d = 2$ corresponds to the glassy Ising spin systems studied in previous studies [20], albeit with a temperature that differs by a factor of two. In Fig. 3, we show the detailed results by Thomas and Katzgraber [36] rescaled appropriately for comparison. Note that this setup is stable up to close to the hashing bound value of $p_{\rm hb} \approx 0.11$, i.e., even if approximately 10.9% of the qubits are faulty, errors can still be corrected.

For qutrits ($d = 3$) without any disorder, the transition occurs at $T_{c,d=3} \approx 1.01(4)$. As the amount of disorder is gradually increased, the transition temperature $T_c(d, p)$ is lowered until it meets the Nishimori line. Because finite-size effect are most pronounced close to the critical error threshold, the error bars calculated by bootstrapping the finite-size scaling analysis are larger. The largest value for which we find a crossing in the two-point finite-size correlation function is $p_{c,d=3} = 0.158(2)$. This means that even when 15.8% of the qutrits in a topological memory are faulty, error correction is still possible and the encoded information is retained. Notably, this numerical estimate agrees with the result previously found by Honecker *et al.* [37], with the disorder defined as $p' = p/(d-1)$. Since the method based on the domain-wall free energy they employ detects the transition at $T = 0$, this also indicates that a possible reentrance effect is small.

For higher-dimensional qudits ($d = 4$, 6 and 10), an analogous analysis indicates that the error threshold for these codes closely traces the hashing bound, Eq. (4), as conjectured in Refs. [38–40]. These findings are summarized in the inset of Fig. 3, which relates the numerical estimates for the error thresholds (data points) to the respective hashing bound value (line). Note that the precision is limited by the numerical sampling effort: The required equilibration time for disordered d-level Potts systems increases dramatically for larger values of d, because the configuration space grows exponentially and the transition temperature is lowered at the same time. However, we do emphasize that the topological stability of qudit-based codes increases monotonically with d, i.e., implementing higher-level qudits leads to increasingly stable topologically protected memory.

V. CONCLUSION

We have demonstrated that error correction in topological memory built from qudits is closely related to the ferromagnetic ordering in classical disordered d-state Potts systems. By numerically estimating the phase boundary for the related classical statistical-mechanical model, we show that error correction remains feasible up to the hashing bound (within error bars) for values of d between 2 and 10. Our results are summarized in Fig. 3, which shows the estimated phase diagram and Nishimori line for all values of d studied. The inset relates the numerical estimates for the error thresholds to the hashing bound, Eq. (4). In particular, our results demonstrate that, by moving from qubit to qutrit building blocks, the resilience of a topological quantum memory can potentially be increased already by at least 42%.

The thresholds we obtain are found to be significantly larger than those obtained by current decoding methods. The highest effective thresholds obtained so far reach to only around 80% of the Hashing bound values [23]. This is due to approximations inherent in the design of these decoders. Our results suggest that there is still progress to be made in their development.

Acknowledgments

The authors would like to thank the Santa Fe Institute for HPC resources on the Scoville cluster, and in particular, N. Metheny for its administration and continued technical support. H.G.K. acknowledges support from the National Science Foundation (Grant No. DMR-1151387) and would like to thank the Santa Fe Institute for their hospitality. J.R.W. acknowledges support from the Swiss National Science Foundation, as well as and NCCR QSIT.

[1] R. Feynman, *Quantum mechanical computers*, Optics news **11**, 1 (1985).

[2] P. W. Shor, *Polynomial-time algorithms for prime factoriza-*

tion and discrete logarithms on a quantum computer, SIAM J. Comp. **26**, 1484 (1997).

[3] P. W. Shor, *Scheme for reducing decoherence in quantum computer memory*, Phys. Rev. A **52**, R2493 (1995).

[4] A. M. Steane, *Error Correcting Codes in Quantum Theory*, Phys. Rev. Lett. **77**, 793 (1996).

[5] H. Bechmann-Pasquinucci and A. Peres, *Quantum cryptography with 3-state systems*, Phys. Rev. Lett. **85**, 3313 (2000).

[6] M. A. Nielsen, M. J. Bremner, J. L. Dodd, A. M. Childs, and C. M. Dawson, *Universal simulation of Hamiltonian dynamics for quantum systems with finite-dimensional state spaces*, Phys. Rev. A **66**, 022317 (2002).

[7] B. P. Lanyon, M. Barbieri, M. P. Almeida, T. Jennewein, T. C. Ralph, K. J. Resch, G. J. Pryde, J. L. O'Brien, A. Gilchrist, and A. G. White, *Simplifying quantum logic using higher-dimensional Hilbert spaces*, Nat. Phys. **5**, 134 (2009).

[8] H. Anwar, E. T. Campbell, and D. E. Browne, *Qutrit magic state distillation*, New J. Phys. **14**, 063006 (2012).

[9] E. T. Campbell, H. Anwar, and D. E. Browne, *Magic-State Distillation in All Prime Dimensions Using Quantum Reed-Muller Codes*, Phys. Rev. X **2**, 041021 (2012).

[10] S. S. Bullock, D. P. O'Leary, and G. K. Brennen, *Asymptotically optimal quantum circuits for d-level systems*, Phys. Rev. Lett. **94**, 230502 (2005).

[11] D. Nigg, M. Mueller, E. A. Martinez, P. Schindler, M. Hennrich, T. Monz, M. A. Martin-Delgado, and R. Blatt, *Experimental Quantum Computations on a Topologically Encoded Qubit* (2014), (arxiv:quant-phys/1403.5426).

[12] A. Mair, A. Vaziri, G. Weihs, and A. Zeilinger, *Entanglement of the orbital angular momentum states of photons*, Nature **412**, 313 (2001).

[13] M. Piani, D. Pitkanen, R. Kaltenbaek, and N. Lütkenhaus, *Linear-optics realization of channels for single-photon multimode qudits*, Phys. Rev. A **84**, 032304 (2011).

[14] M. Neeley, M. Ansmann, R. C. Bialczak, M. Hofheinz, E. Lucero, A. D. O'Connell, D. Sank, H. Wang, J. Wenner, A. N. Cleland, et al., *Emulation of a Quantum Spin with a Superconducting Phase Qudit*, Science **325**, 722 (2009).

[15] A. B. Klimov, R. Guzmán, J. C. Retamal, and C. Saavedra, *Qutrit quantum computer with trapped ions*, Phys. Rev. A **67**, 062313 (2003).

[16] B. E. Mischuck, S. T. Merkel, and I. H. Deutsch, *Control of inhomogeneous atomic ensembles of hyperfine qudits*, Phys. Rev. A **85**, 022302 (2012).

[17] A. Y. Kitaev, *Fault-tolerant quantum computation by anyons*, Ann. Phys. **303**, 2 (2003).

[18] H. Bombin and M. A. Martin-Delgado, *Topological Quantum Distillation*, Phys. Rev. Lett. **97**, 180501 (2006).

[19] S. S. Bullock and G. K. Brennen, *Qudit surface codes and gauge theory with finite cyclic groups*, J. Phys. A **40**, 3481 (2007).

[20] E. Dennis, A. Kitaev, A. Landahl, and J. Preskill, *Topological quantum memory*, J. Math. Phys. **43**, 4452 (2002).

[21] H. G. Katzgraber, H. Bombin, R. S. Andrist, and M. A. Martin-Delgado, *Topological color codes on Union Jack lattices: a stable implementation of the whole Clifford group*, Phys. Rev. A **81**, 012319 (2010).

[22] R. S. Andrist, H. G. Katzgraber, H. Bombin, and M. A. Martin-Delgado, *Tricolored Lattice Gauge Theory with Randomness: Fault-Tolerance in Topological Color Codes*, New J. Phys. **13**, 083006 (2011).

[23] G. Duclos-Cianci and D. Poulin, *Kitaev's $\mathbb{Z}_d$-code threshold estimates*, Phys. Rev. A. **87**, 062338 (2013).

[24] H. Anwar, B. J. Brown, E. T. Campbell, and D. E. Browne, *Efficient Decoders for Qudit Topological Codes* (2013), (arXiv/quant-ph:1311.4895).

[25] A. Hutter, D. Loss, and J. R. Wootton, *Improved HDRG decoders for qudit and non-Abelian quantum error correction* (2014), (arXiv:1410.4478).

[26] B. Röthlisberger, J. R. Wootton, R. M. Heath, J. K. Pachos, and D. Loss, *Incoherent dynamics in the toric code subject to disorder*, Phys. Rev. A **85**, 022313 (2012).

[27] H. Bombin, R. S. Andrist, M. Ohzeki, H. G. Katzgraber, and M. A. Martin-Delgado, *Strong Resilience of Topological Codes to Depolarization*, Phys. Rev. X **2**, 021004 (2012).

[28] S. Lloyd, *Capacity of the noisy quantum channel*, Phys. Rev. A **55**, 1613 (1997).

[29] I. Devetak, *The private classical capacity and quantum capacity of a quantum channel*, Information Theory, IEEE Transactions on **51**, 44 (2005).

[30] H. Nishimori, *Internal Energy, Specific Heat and Correlation Function of the Bond-Random Ising Model*, Prog. Theor. Phys. **66**, 1169 (1981).

[31] K. Hukushima and K. Nemoto, *Exchange Monte Carlo method and application to spin glass simulations*, J. Phys. Soc. Jpn. **65**, 1604 (1996).

[32] M. E. J. Newman and G. T. Barkema, *Monte Carlo Methods in Statistical Physics* (Oxford University Press Inc., New York, USA, 1999).

[33] H. G. Katzgraber, S. Trebst, D. A. Huse, and M. Troyer, *Feedback-optimized parallel tempering Monte Carlo*, J. Stat. Mech. P03018 (2006).

[34] M. Palassini and S. Caracciolo, *Universal Finite-Size Scaling Functions in the 3D Ising Spin Glass*, Phys. Rev. Lett. **82**, 5128 (1999).

[35] H. G. Katzgraber, H. Bombin, and M. A. Martin-Delgado, *Error Threshold for Color Codes and Random 3-Body Ising Models*, Phys. Rev. Lett. **103**, 090501 (2009).

[36] C. K. Thomas and H. G. Katzgraber, *Simplest model to study reentrance in physical systems*, Phys. Rev. E **84**, 040101(R) (2011).

[37] A. Honecker, J. L. Jacobsen, M. Picco, and P. Pujol, *Nishimori Point in Random-Bond Ising and Potts Models in 2D* (2001), (arXiv:cont-mat/0112069v1).

[38] H. Nishimori and K. Nemoto, *Duality and Multicritical Point of Two-Dimensional Spin Glasses*, J. Phys. Soc. Jpn. **71**, 1198 (2002).

[39] J.-M. Maillard, K. Nemoto, and H. Nishimori, *Symmetry, complexity and multicritical point of the two-dimensional spin glass*, J. Phys. A **36**, 9799 (2003).

[40] M. Ohzeki, *Precise locations of multicritical points for spin glasses on regular lattices*, Phys. Rev. E **79**, 021129 (2009).

[41] We are not aware of a physical motivation explicitely favoring this method for extrapolation to the thermodynamic limit, apart from its simplicity (limiting bias / overfitting) and historically proven applicability (the data for several parametrized disordered models of this type have been shown to fall on a line when plotted as a function of the inverse system size). When plotting the crossings $T_c^*(L_1, L_2)$ for a fixed ratio of e.g. $L_1 = 2L_2$ against $1/L_1$, the y-intercept correponds to the limit value $\lim_{L_1\to\infty} T_c^* \doteq T_c$. The choice of $2/(L_1{+}L_2)$ here merely allows us to use the crossings for varying system size ratios in the extrapolation, while still being proportional to $1/L_1$ for fixed system size ratios.